

Semileptonic  $B_c \rightarrow \eta_c, J/\psi$  transitionsZhao-Qian Yao<sup>a,b</sup>, Daniele Binosi<sup>c</sup>, Zhu-Fang Cui<sup>a,b</sup>, Craig D. Roberts<sup>a,b,\*</sup><sup>a</sup> School of Physics, Nanjing University, Nanjing, Jiangsu 210093, China<sup>b</sup> Institute for Nonperturbative Physics, Nanjing University, Nanjing, Jiangsu 210093, China<sup>c</sup> European Centre for Theoretical Studies in Nuclear Physics and Related Areas, Villa Tambosi, Strada delle Tabarelle 286, I-38123 Villazzano (TN), Italy

## Abstract

Using a systematic, symmetry-preserving continuum approach to the Standard Model strong-interaction bound-state problem, we deliver parameter-free predictions for all semileptonic  $B_c \rightarrow \eta_c, J/\psi$  transition form factors on the complete domains of empirically accessible momentum transfers. Working with branching fractions calculated therefrom, the following values of the ratios for  $\tau$  over  $\mu$  final states are obtained:  $R_{\eta_c} = 0.313(22)$  and  $R_{J/\psi} = 0.242(47)$ . Combined with other recent results, our analysis confirms a  $2\sigma$  discrepancy between the Standard Model prediction for  $R_{J/\psi}$  and the single available experimental result.

2021 April 18

**Keywords:** heavy-quark mesons, semileptonic decays, charmonia, CKM matrix elements, emergence of hadron mass, Schwinger function methods

## 1. Introduction

The  $B_c$  meson was discovered a little over twenty years ago [1]. With mass  $m_{B_c} = 6.2749(8)$  GeV [2], it lies below the threshold for  $BD$  decay; and since it is an open flavour state, electromagnetic decays are forbidden. Thus, within the Standard Model, only flavour-changing weak decays are possible. Consequently,  $B_c$  has a relatively long lifetime [2]:

$$0.510(9) \text{ ps}, \quad (1)$$

which is, *e.g.* ten-billion-times longer than that of the  $\eta_c$ . These things make the  $B_c$  an especially interesting system: it is the lightest open-flavour bound-state of the two heaviest quarks in Nature that are experimentally pliable; and lives long enough to make measurements possible.

Flavour-changing  $B_c$  weak decays involve one of the following transitions:  $\bar{b} \rightarrow \bar{u}, \bar{b} \rightarrow \bar{c}, c \rightarrow s, c \rightarrow d$ . Specific entries in the Cabbibo-Kobayashi-Maskawa (CKM) matrix modulate the strengths of these transitions. Since  $|V_{cs}|$  is the largest of the four that can be involved here, one may anticipate that  $B_c \rightarrow B_s$  transitions dominate. This expectation is supported by contemporary calculations, *e.g.* Refs. [3–5]. Another factor is the available phase space. For instance, with  $\eta_c, J/\psi$  final states, this is more than ten-times larger than for  $B$ ; and such magnification may be sufficient to overwhelm the factor of roughly six suppression from  $|V_{cb}|/|V_{cd}|$ . Calculations of the branching fractions ratio bear this out, *e.g.* [5]:  $\mathcal{B}_{B_c^+ \rightarrow \eta_c \ell^+ \nu} / \mathcal{B}_{B_c^+ \rightarrow B^0 \ell^+ \nu} \approx 6$ , where  $\ell$  is a light lepton. (This is a longstanding qualitative prediction [6, 7].) Therefore, it is not surprising that the  $B_c$  was discovered in decays to  $J/\psi$  final states, especially given the narrow, prominent decay width for  $J/\psi \rightarrow \ell^+ \ell^-$ .

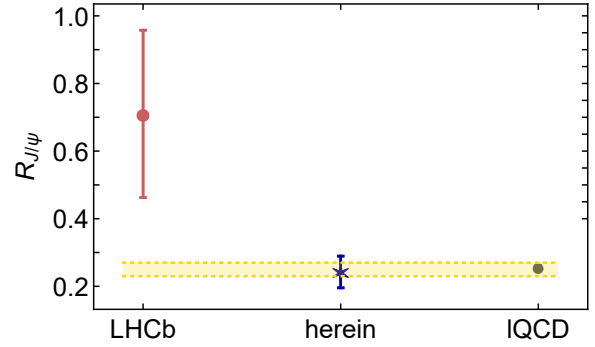


Figure 1: Ratio  $R_{J/\psi}$  in Eq. (2) – red circle, empirical result from LHCb Collaboration [8]; blue star – our prediction; grey square – IQCD result [9, 10]; and gold band – unweighted mean of central values from contemporary calculations [11–16] (Details provided below in connection with Table 5B.)

Data acquired in the last decade, potentially indicating violations of lepton universality in  $b$ -quark decays [17–23], raise studies of the semileptonic decays of  $B_c$ -mesons with ground-state charmonia final-states to a new level of importance in the search for physics outside the Standard Model paradigm. In fact, the LHCb collaboration has reported [8]:

$$R_{J/\psi} := \frac{\mathcal{B}_{B_c^+ \rightarrow J/\psi \tau \nu}}{\mathcal{B}_{B_c^+ \rightarrow J/\psi \mu \nu}} = 0.71 \pm 0.17 \text{ (stat)} \pm 0.18 \text{ (syst)} \quad (2)$$

and stated that this result lies approximately two standard-deviations ( $2\sigma$ ) above the range of central values predicted by reliable calculations within the Standard Model, as highlighted by Fig. 1. Such a discrepancy could signal violation of lepton universality in Nature’s weak interactions.

\*Corresponding Author

Email addresses: zqyao@mail.nju.edu.cn (Zhao-Qian Yao),

binosi@ectstar.eu (Daniele Binosi), phycui@nju.edu.cn (Zhu-Fang Cui), cdroberts@nju.edu.cn (Craig D. Roberts)

Following early calculations [6], numerous methods have been employed in the analysis of  $B_c \rightarrow \eta_c, J/\psi$  semileptonic decays; and amongst the more recent are an array of continuum studies [11–16, 24, 25] and first results from lattice-regularised QCD (LQCD) [9, 10, 26]. We tackle the problem using a framework that is distinct from all these. Namely, a continuum Schwinger function method (CSM) for solving hadron bound-state problems [27–30], which has provided a unified explanation for the properties of mesons and baryons with 0–3 heavy quarks, *i.e.* from Nature’s (almost) Nambu-Goldstone bosons to triply-heavy baryons; see *e.g.* Refs. [31–40].

## 2. Transition Form Factors: Definitions

We consider the following transition matrix elements:

$$\begin{aligned} M_\mu^{B_c \rightarrow \eta_c}(P, Q) &= \langle \eta_c(p_{\eta_c}) | \bar{c} i \gamma_\mu b | B_c(k) \rangle \\ &= f_+(t) T_{\mu\nu}^Q P_\nu + f_0(t) \frac{P \cdot Q}{Q^2} Q_\mu, \end{aligned} \quad (3a)$$

$$\begin{aligned} M_{\mu;\lambda}^{B_c \rightarrow J/\psi}(P, Q) &= \langle \psi^\lambda(p_\psi; \lambda) | \bar{c} i (\gamma_\mu - \gamma_\mu \gamma_5) b | B_c(k) \rangle \\ &= 2m_{J/\psi} \frac{Q_\mu \epsilon^\lambda \cdot Q}{Q^2} A_0(t) + [m_{B_c} + m_{J/\psi}] T_{\mu\nu}^Q \epsilon_\nu^\lambda A_1(t) \\ &\quad + [P_\mu + Q_\mu \frac{m_{B_c}^2 - m_{J/\psi}^2}{Q^2}] \frac{\epsilon^\lambda \cdot Q A_2(t)}{m_{B_c} + m_{J/\psi}} \\ &\quad + \epsilon_{\mu\nu\rho\sigma} \epsilon_\nu^\lambda k_\rho P_\psi^\sigma \frac{2V(t)}{m_{B_c} + m_{J/\psi}}, \end{aligned} \quad (3b)$$

where  $Q^2 T_{\mu\nu}^Q = Q^2 \delta_{\mu\nu} - Q_\mu Q_\nu$ ,  $P = k + p_{\eta_c, \psi}$ ,  $Q = p_{\eta_c, \psi} - k$ , with  $k^2 = -m_{B_c}^2$  and  $p_{\eta_c}^2 = -m_{\eta_c}^2$ ,  $p_\psi^2 = -m_{J/\psi}^2$ ;  $\epsilon_\nu^\lambda(p_f)$  is a polarisation four-vector, with  $\sum_{\lambda=1}^3 \epsilon_\nu^\lambda(p_f) \epsilon_\mu^\lambda(p_f) = T_{\mu\nu}^{p_f}$ ; the squared-momentum-transfer is  $t = -Q^2$ ; and  $t_\pm^M = (m_{B_c} \pm m_M)^2$ ,  $M = \eta_c, J/\psi$ . ( $t_-$  is the largest accessible value of  $t$  in the identified physical decay process.) The scalar functions in Eqs. (3) are the semileptonic transition form factors, which express all effects of hadron structure on the transitions. Ensuring the absence of kinematic singularities in Eqs. (3), symmetries require

$$f_+(0) = f_0(0), \quad (4a)$$

$$A_0(0) = \frac{m_{B_c} + m_{J/\psi}}{2m_{J/\psi}} A_1(0) - \frac{m_{B_c} - m_{J/\psi}}{2m_{J/\psi}} A_2(0). \quad (4b)$$

With predictions for the transition form factors in hand, one can compute the associated decay branching fractions from the differential decay width for  $B_c \rightarrow M \ell^+ \nu_\ell$ :

$$\frac{d\Gamma}{dt} \Big|_{B_c \rightarrow M \ell^+ \nu_\ell} = \frac{G_F^2 |V_{cb}|^2}{192\pi^3 m_{B_c}^3} \lambda(m_{B_c}, m_M, t) \frac{(t - m_\ell^2)^2}{t^2} \mathcal{H}^2, \quad (5)$$

where:  $G_F = 1.166 \times 10^{-5} \text{ GeV}^{-2}$ ;  $|V_{cb}| = 0.0410(14)$  [2];  $\lambda(m_{B_c}, m_M, t)^2 = (t_+ - t)(t_- - t)$ ;

$$\mathcal{H}^2 = (H_+^2 + H_-^2 + H_0^2) \left(1 + \frac{m_\ell^2}{2t}\right) + \frac{3m_\ell^2}{2t} H_t^2, \quad (6)$$

$m_\ell^2 \leq t \leq t_-$ ,  $m_\ell$  is the lepton mass. For  $M = \eta_c$ ,  $H_\pm \equiv 0$ ,

$$H_0 = \lambda(m_{B_c}, m_{\eta_c}, t) f_+(t), \quad H_t = (m_{B_c}^2 - m_{\eta_c}^2) f_0(t); \quad (7)$$

whereas when  $M = J/\psi$ ,

$$\frac{1}{\sqrt{t}} H_\pm = (m_{B_c} + m_{J/\psi}) A_1(t) \mp \frac{\lambda(m_{B_c}, m_{J/\psi}, t)}{m_{B_c} + m_{J/\psi}} V(t), \quad (8a)$$

$$\begin{aligned} H_0 &= \frac{1}{2m_{J/\psi}} \left[ (m_{B_c}^2 - m_{J/\psi}^2 - t)(m_{B_c} + m_{J/\psi}) A_1(t) \right. \\ &\quad \left. - \frac{\lambda(m_{B_c}, m_{J/\psi}, t)^2}{m_{B_c} + m_{J/\psi}} A_2(t) \right], \end{aligned} \quad (8b)$$

$$H_t = \lambda(m_{B_c}, m_{J/\psi}, t) A_0(t). \quad (8c)$$

After integrating Eq. (5) to obtain the required partial widths, one quotes the branching fractions,  $\mathcal{B}_{B_c \rightarrow M \ell^+ \nu_\ell}$ , with respect to the total width determined from Eq. (1).

## 3. Transition Form Factors: Matrix Elements

At leading-order (rainbow-ladder, RL) in the most widely used CSM truncation [41, 42], which has been employed to unify, *inter alia*, all semileptonic pseudoscalar-to-pseudoscalar transitions involving  $\pi, K, D_{(s)}$  initial states [40, 43], the matrix elements in Eqs. (3) take the following form:

$$\begin{aligned} M_\mu^{B_c \rightarrow M}(P, Q) &= N_c \text{tr} \int \frac{d^4 s}{(2\pi)^4} S_b(s-k) \Gamma_{B_c}(s-k/2; k) S_c(s) \\ &\quad \times \Gamma_M(s-p/2; -p) S_c(s-p) i \mathcal{W}_\mu^{cb}(s-p, s-k), \end{aligned} \quad (9)$$

where  $N_c = 3$  and the trace is over spinor indices. There are three types of matrix-valued functions in Eq. (9). The simplest are the propagators for the dressed-quarks involved in the transition process:  $S_f(s)$ ,  $f = c, b$ ; then there are the Bethe-Salpeter amplitudes for the mesons involved:  $\Gamma_M$ ; and, finally, the dressed  $b \rightarrow c$  weak transition vertex:  $\mathcal{W}_\mu^{bc}$ . Each of these quantities can be computed once the kernel of the RL Bethe-Salpeter equation is specified. Importantly, Eq. (9) preserves the identities in Eqs. (4), both algebraically and numerically.

With a realistic kernel, RL truncation provides a sound description of systems wherein [30]: (i) orbital angular momentum does not play a large role and (ii) the non-Abelian anomaly can be neglected. In such cases, corrections to the truncation largely cancel amongst themselves.  $\eta_c, J/\psi, B_c$  are amongst the systems for which these conditions hold. Herein, we use the RL kernel detailed in Refs. [31–33]:

$$\mathcal{K}_{\rho_1 \rho'_1, \rho_2 \rho'_2} = \mathcal{G}_{\mu\nu}(k) [i \gamma_\mu]_{\rho_1 \rho'_1} [i \gamma_\nu]_{\rho_2 \rho'_2}, \quad (10a)$$

$$\mathcal{G}_{\mu\nu}(k) = \tilde{\mathcal{G}}(k^2) T_{\mu\nu}^k, \quad (10b)$$

with ( $s = k^2$ )

$$\tilde{\mathcal{G}}(s) = \frac{8\pi^2}{\omega^4} D e^{-s/\omega^2} + \frac{8\pi^2 \gamma_m \mathcal{F}(s)}{\ln[\tau + (1 + s/\Lambda_{\text{QCD}}^2)]}, \quad (11)$$

where  $\gamma_m = 4/\beta_0$ ,  $\beta_0 = 11 - (2/3)n_f$ ,  $n_f = 5$ ,  $\Lambda_{\text{QCD}} = 0.36 \text{ GeV}$ ,  $\tau = e^2 - 1$ , and  $\mathcal{F}(s) = \{1 - \exp(-s/[4m_t^2])\}/s$ ,  $m_t = 0.5 \text{ GeV}$ . Following standard practice, in solving all integral equations [44], we use a mass-independent momentum-subtraction renormalisation scheme, fixing each renormalisation constant in the chiral limit, with renormalisation scale  $\zeta = 19 \text{ GeV} =: \zeta_{19}$ .

Table 1: Static properties of mesons evaluated using bound-state equations defined by the kernel specified in Eqs. (10), (11). Normalisation: the empirical value of the pion’s leptonic decay constant is  $f_\pi \approx 0.092$  GeV. Empirical values (expt.), where available, drawn from Ref. [2]; and lattice-QCD (lQCD) results for leptonic decay constants from Refs. [51–53]. The mean absolute relative error between our predictions and empirical results is 3.6%. (All dimensioned quantities in GeV.)

	$m_{\eta_c}$	$m_{J/\psi}$	$m_{B_c}$	$m_{\eta_b}$	$m_\Upsilon$	$f_{\eta_c}$	$f_{J/\psi}$	$f_{B_c}$	$f_{\eta_b}$	$f_\Upsilon$
herein	2.98	3.12	6.27	9.19	9.28	0.28	0.30	0.43	0.56	0.53
expt.	2.98	3.10	6.27	9.40	9.46	0.24	0.29			0.51
lQCD						0.28	0.29	0.31	0.47	0.46

The elaboration of Eqs. (10), (11) and their connection with QCD are described in Refs. [31, 32, 34]. Here, we simply reiterate some points. (i) The interaction is consistent with that found through studies of QCD’s gauge sector, capitalising on the fact that the gluon propagator is a bounded, smooth function of spacelike momenta, which achieves its maximum value on this domain at  $s = 0$  [45–47]; and the dressed gluon-quark vertex does not possess any structure which can qualitatively alter these features [48]. (ii) It is specified in Landau gauge because, *inter alia*, this gauge is a fixed point of the renormalisation group and ensures that sensitivity to the form of the gluon-quark vertex is minimal, thus providing the conditions for which RL truncation is most accurate. (iii) The interaction preserves the one-loop renormalisation group behaviour of QCD; hence, *e.g.* the quark mass-functions produced are independent of the renormalisation point. (iv) On  $s \lesssim (2m_t)^2$ , Eq. (11) defines a two-parameter *Ansatz*, the details of which determine whether such corollaries of emergent hadron mass as confinement and dynamical chiral symmetry breaking are realised in solutions of the bound-state equations [49, 50].

The analyses in Ref. [33] determined that one can unify the properties of a diverse range of systems using  $\omega = 0.8$  GeV,  $\zeta^3 = D\omega = (0.6 \text{ GeV})^3$  and we use these values hereafter. An additional feature of Eq. (11) is that with a given value of  $\zeta$ , results for observable quantities are practically insensitive to variations  $\omega \rightarrow \omega(1 \pm 0.1)$ ; so, there is no issue of fine tuning.

We now illustrate the qualities of the framework by computing an array of heavy pseudoscalar meson static properties, *i.e.* their masses and leptonic decay constants. Solving the gap and Bethe-Salpeter equations (see, *e.g.* Ref. [39] and Ref. [40, Appendix 1]) with the following values of the renormalisation-point-invariant  $c$  and  $b$  current-quark masses (in GeV):

$$\hat{m}_c = 1.61, \quad \hat{m}_b = 6.96, \quad (12)$$

one obtains the results in Table 1. The mean absolute relative error between our predictions and empirical values is 3.6%. For later use, we note that  $r_{b;c} = \hat{m}_b/\hat{m}_c = 4.32$  and, equivalently,  $r_{c;b} = 0.23$ .

The masses in Eq. (12) correspond to the following current masses at our renormalisation scale:  $m_c^{\zeta^{19}} = 0.82$  GeV,  $m_b^{\zeta^{19}} = 3.55$  GeV; and one-loop evolved to  $\zeta = \zeta_2 = 2$  GeV,  $m_c^{\zeta_2} = 1.22$  GeV,  $m_b^{\zeta_2} = 5.26$  GeV. Working with the dressed-quark mass-functions obtained by solving the gap equations,

$M_{c,b}(k)$ , and defining Euclidean constituent-quark masses as the solutions of  $M_{c,b}(M_{c,b}^E) = M_{c,b}^E$ , one finds (in GeV):

$$M_c^E = 1.33, \quad M_b^E = 4.12. \quad (13)$$

These quantities are analogous to the “running masses” often quoted in connection with heavy quarks and our predictions are within 3% of those listed elsewhere [2].

It is worth remarking on some important physical aspects of the weak transition vertex,  $\mathcal{W}_\mu^{cb}$ . Pseudoscalar-to-pseudoscalar transitions only involve the vector part, which possesses poles at  $Q^2 + m_{B_c, B_{c0}}^2 = 0$ . Pseudoscalar-to-vector transitions also involve the axial-vector part. This has poles at  $Q^2 + m_{B_c, B_{c1}}^2 = 0$ . The presence of these poles is a prerequisite for any valid analysis of  $B_c \rightarrow \eta_c, J/\psi$  semileptonic transitions. They are manifest in our treatment.

#### 4. Computational Scheme and Results

The integration in Eq. (9) samples the appearing functions on a material domain of their complex-valued arguments. So long as the masses of the initial and final state mesons are similar, *i.e.* the ratio of the current-masses of the quarks involved,  $r_{Q_1:Q_2}$ , does not differ too much from unity, the integral can readily be evaluated using simple numerical techniques because  $t_-$  and, hence, the maximum momentum of the recoiling meson, remains modest. However, at some value of  $r_{Q_1:Q_2} =: r_f, t_-$  becomes so large that singularities associated with the analytic structure of the dressed-quark propagators [54, 55] move into the complex- $s^2$  integration domain and straightforward numerical techniques fail.

This sort of problem was solved in Ref. [56] by using perturbation theory integral representations (PTIRs) [57] for each matrix-valued function in the integrand defining the associated matrix element. However, constructing accurate PTIRs is time consuming; and here the challenge is compounded because the complete set of integrands involves 46 distinct scalar functions. Like Ref. [40], we therefore adopt a different approach.

(I) – We consider the semileptonic transitions of a fictitious  $c\bar{Q}$  pseudoscalar meson:  $B_{c\bar{Q}} \rightarrow \eta_{c\bar{c}}, J/\psi_{c\bar{c}}$ . All relevant Schwinger functions and, subsequently, the transition form factors are computed as a function of  $\hat{m}_Q$  as it is increased from the point  $r_{Q;c} = 1$  to  $r_f^{\eta_c} = 3.17$  or  $r_f^{J/\psi} = 2.93$ . Then, using the statistical Schlessinger point method (SPM), exploited successfully elsewhere [37, 39, 58–65], we build  $\hat{m}_Q$ -interpolations of all transition form factors, which are then used to extrapolate every measurable feature of the matrix elements to the physical point  $r_{b;c} = 4.32$ , Eq. (12).

(II) – These exercises are repeated from an inverted perspective. To wit, beginning with an analogous initial state, we consider  $B_{Q\bar{b}} \rightarrow \eta_{Q\bar{Q}}, J/\psi_{Q\bar{Q}}$ , where the final states are  $Q\bar{Q}$  mesons, with  $\eta_c, J/\psi$  quantum numbers. The transition form factors are then computed as a function of  $\hat{m}_Q$ , reducing it from the point  $r_{Q;b} = 1$  to  $r_f^{\eta_{Q\bar{Q}}} = 0.56$  or  $r_f^{J/\psi_{Q\bar{Q}}} = 0.63$ . SPM extrapolation is subsequently used to reach the physical value,  $r_{c;b} = 0.23$ , Eq. (12). Since extrapolations of initial and final states are required here, the SPM uncertainty is larger.

Table 2: *Panels A-F.* SPM interpolation parameters for each transition form factor considered herein, as labelled: Eq. (15),  $\alpha_1$  is dimensionless and  $\alpha_{2,3}$  have dimension  $\text{GeV}^{-1}$ . *N.B.* Regarding  $f_{+,0}^{B_c \rightarrow \eta_c}$ ,  $\alpha_1$  is the same in both cases because  $f_+(0) = f_0(0)$ . (The SPM uncertainty estimate is discussed in the paragraph before that containing Eq. (14).)

(A) $f_+^{B_c \rightarrow \eta_c}$	$\alpha_1$	$\alpha_2$	$\alpha_3$
SPM (I)	0.634(07)	0.0327(05)	0.0550(08)
SPM (II)	0.630(17)	0.0318(33)	0.0659(16)
mean (III)	0.632(13)	0.0323(24)	0.0605(13)
(B) $f_0^{B_c \rightarrow \eta_c}$	$\alpha_1$	$\alpha_2$	$\alpha_3$
SPM (I)	0.634(07)	0.0243(08)	0.0328(7)
SPM (II)	0.630(17)	0.0258(14)	0.0352(6)
mean (III)	0.632(13)	0.0251(11)	0.0340(7)
(C) $A_0^{B_c \rightarrow J/\psi}$	$\alpha_1$	$\alpha_2$	$\alpha_3$
SPM (I)	0.563(13)	0.0331(21)	0.0572(049)
SPM (II)	0.586(44)	0.0269(58)	0.0531(110)
mean (III)	0.574(33)	0.0300(43)	0.0552(085)
(D) $A_1^{B_c \rightarrow J/\psi}$	$\alpha_1$	$\alpha_2$	$\alpha_3$
SPM (I)	0.546(19)	0.0175(29)	0.0238(54)
SPM (II)	0.557(29)	0.0199(45)	0.0488(68)
mean (III)	0.551(25)	0.0187(38)	0.0363(61)
(E) $A_2^{B_c \rightarrow J/\psi}$	$\alpha_1$	$\alpha_2$	$\alpha_3$
SPM (I)	0.546(11)	0.0197(43)	0.0508(68)
SPM (II)	0.576(38)	0.0213(24)	0.0238(86)
mean (III)	0.561(28)	0.0205(35)	0.0373(77)
(F) $V^{B_c \rightarrow J/\psi}$	$\alpha_1$	$\alpha_2$	$\alpha_3$
SPM (I)	0.827(26)	0.0439(54)	0.0350(135)
SPM (II)	0.845(51)	0.0463(99)	0.0210(088)
mean (III)	0.836(41)	0.0451(80)	0.0280(110)

(III) – Having completed these exercises, we combine the outcomes to produce our final results.

It is worth remarking that the SPM is founded on interpolation via continued fractions [66, 67]. It is typically augmented today by statistical sampling. The approach avoids any assumptions on the function used for the representation of input and captures both local and global features of that source. This latter aspect underpins the reliability of subsequent extrapolations. The SPM can accurately reconstitute a complex-valued function within a radius of convergence determined by that one of the function’s branch points which lies nearest the real domain from which the sample points are drawn. The statistical aspect ensures that one has a genuine estimate of the uncertainty associated with any extrapolation.

To elucidate further, we first compute the value of a given quantity,  $\mathcal{X}$ , at  $N = 40$  different values of the evolving mass,  $\hat{m}_Q$ , distributed evenly on the domain of direct computation. Then,  $M = 20$  values of  $\hat{m}_Q$  are chosen at random from this 40-element set, using which a continued fraction interpolation is developed for  $\mathcal{X}(\hat{m}_Q)$  on this 20-element subset. A large number of interpolating functions,  $n_I$ , is subsequently obtained by

Table 3: SPM predictions for meson masses (in GeV) that determine the locations of the timelike pole in the transition form factors computed herein, Eq. (15). These masses have not yet been measured; so, we present IQCD results for context [68]. (The SPM uncertainty estimate is discussed in the paragraph before that containing Eq. (14).)

	$m_{B_c^*}$	$m_{B_{c0}^*}$	$m_{B_{c1}}$
SPM (I)	6.402(20)	6.767(21)	6.880(20)
SPM (II)	6.382(26)	6.752(28)	6.851(26)
mean (III)	6.392(23)	6.760(25)	6.866(23)
IQCD	6.331(07)	6.712(19)	6.736(18)

inspecting the  $C(N, M)$  combinatorial possibilities for the  $M$  element subset and eliminating those functions which fail to satisfy a simple physical constraint; namely, we insist that each interpolation be smooth on the domain of required current-quark masses. For all quantities considered, this constraint yields  $n_I \approx 100,000$  acceptable interpolations. Our prediction for  $\mathcal{X}$  is then obtained by extrapolating each of the associated  $n_I$  physical SPM interpolants to the target current-mass and reporting as the result that value which sits at the centre of the band within which 68% of the interpolants lie. This  $1\sigma$  band is quoted as the uncertainty in the result.

The reliability of our SPM procedure is readily illustrated. The meson masses in Table 1 were computed directly via the Bethe-Salpeter equation using the masses in Eq. (12). One may equally compute masses using the procedures described in (I) and (II) above. Using (I) on  $r_f^{l_{QQ}} \leq r_{Q;b} \leq 1$ , we find  $m_{B_c} = 6.259(1) \text{ GeV}$ ; and employing (II) on  $1 \leq r_{Q;c} \leq r_f^{l_c}$ ,  $m_{B_c} = 6.281(6) \text{ GeV}$ . Hence, the final SPM result is

$$m_{B_c} = 6.270(4) \text{ GeV}, \quad (14)$$

matching the directly computed value in Table 1. Repeating this exercise using the limiting current-masses in the  $J/\psi$  channel, the SPM result is 6.267(8) GeV, again agreeing with Table 1.

On the physical domain associated with any value of  $r_{Q_l:Q_2}$ , each of the transition form factors can accurately be interpolated using the following function:

$$f(t) = \alpha_1 + \alpha_2 t + \frac{\alpha_3 t^2}{m^2 - t}, \quad (15)$$

where  $\alpha_{1,2,3}$  and  $m$  are functions of  $r_{Q;b}$  or  $r_{Q;c}$ . It is the coefficients  $\alpha_{1,2,3}$  for which we develop SPM interpolations. The results are listed in Table 2.

As noted in closing Sec. 2, the pole masses in Eq. (15) correspond to particular mesons:  $f = A_0$ , then  $m = m_{B_c}$ ;  $f = f_+, V$ , then  $m = m_{B_c^*}$ ;  $f = f_0$ , then  $m = m_{B_{c0}^*}$ ; and  $f = A_{1,2}$ , then  $m = m_{B_{c1}}$ . Recall that the first of these masses was calculated directly, with the result in Table 1. The last three can be obtained by analysing the appropriate homogeneous Bethe-Salpeter equations using our SPM method. The results are listed in Table 3. Comparing our predictions with extant IQCD results [68], the mean absolute relative difference is 1.2(0.6)%. Looking closer, we find  $m_{B_{c0}^*} - m_{B_c^*} = 0.368(13) \text{ GeV}$ ,



Table 4: Maximum recoil ( $t = 0$ ) value of each transition form factor calculated herein. Comparisons are provided with other recent analyses: quark model (QM) [11, 12]; phenomenology (ph) [13]; sum rules (SR) [14] modelling based on perturbative QCD (mpQCD) [15]; Salpeter equation (iBS) [16]; and IQCD [10, 26]. As additional context, we list unweighted average values for each of the quantities, evaluated with our prediction excluded (mean-e) and included (mean-i).

	$f_+^{B_c \rightarrow \eta_c}$	$A_0^{B_c \rightarrow J/\psi}$	$A_1^{B_c \rightarrow J/\psi}$	$A_2^{B_c \rightarrow J/\psi}$	$V^{B_c \rightarrow J/\psi}$
herein	0.63(1)	0.57(3)	0.55(3)	0.56(3)	0.84(4)
QM [11, 12]	0.75	0.56	0.55	0.56	0.78
ph [13]	0.56	0.48	0.46	0.49	0.70
SR [14]	0.62(5)	0.54(4)	0.55(4)	0.35(3)	0.73(6)
mpQCD [15]	0.56(7)	0.40(5)	0.47(5)	0.62(6)	0.75(9)
iBS [16]	0.41	0.46	0.48	0.54	0.63
IQCD [26]	0.59(1)		0.49(3)		0.70(2)
IQCD [10]		0.48(3)	0.47(3)	0.48(8)	0.73(7)
mean-e	0.58(11)	0.49(6)	0.50(4)	0.51(9)	0.72(5)
mean-i	0.59(10)	0.50(6)	0.50(4)	0.51(9)	0.73(6)

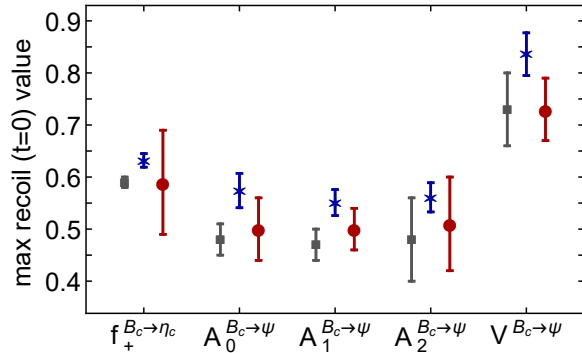


Figure 2: Predicted values of all transition form factors at the maximum recoil point ( $t = 0$ ) – blue stars. Comparisons: IQCD results [10, 26] – grey squares; and unweighted average of each column in Table 4 – red circles.

$m_{B_{c1}} - m_{B_c^*} = 0.474(05) \text{ GeV}$  to be compared with the analogous IQCD results  $0.381(20) \text{ GeV}$ ,  $0.405(19) \text{ GeV}$ . The primary differences are that our prediction for  $m_{B_c^*}$  is 1% larger than the IQCD result and the axial-vector–vector mass-splitting is 17(6)% larger. Considering known empirical masses [2], the mean  $1^{++} - 1^{--}$  mass-splitting is  $0.416(45) \text{ GeV}$ . Our result for  $m_{B_{c1}} - m_{B_c^*}$  is 15(11)% bigger than this. It may, therefore, be an overestimate.

## 5. Transition Form Factors: Predictions and Comparisons

Our predictions for the  $B_c \rightarrow \eta_c$  semileptonic transition form factors are given by Eq. (15) combined with the appropriate masses in Tables 1, 3 and coefficients listed in Table 2. The maximum recoil ( $t = 0$ ) value of each form factor is listed in Table 4, compared with recent continuum and lattice estimates. Aspects of the information in Table 4 are depicted in Fig. 2. Evidently, different approaches produce a range of values for  $f_+(0)$ ; nevertheless, all values fall within  $\lesssim 20\%$  of the mean.

Our  $B_c \rightarrow \eta_c$  transition form factors are drawn in Figs. 3. The difference between these predictions and the preliminary IQCD

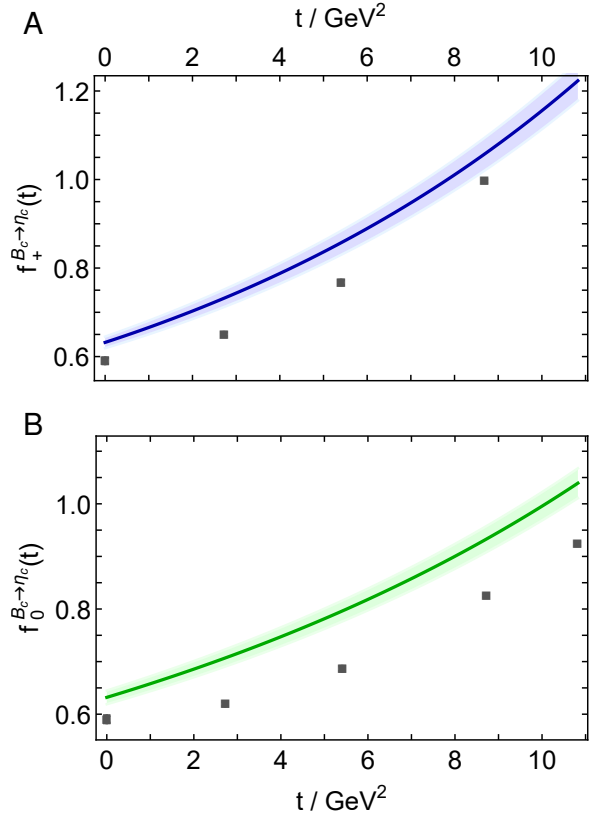


Figure 3: Predicted  $B_c \rightarrow \eta_c$  semileptonic transition form factors. (The shaded bands surrounding each curve express the SPM uncertainty, determined as discussed in the paragraph before that containing Eq. (14).) The points in both panels are preliminary IQCD results from Ref. [26].

results reported in Ref. [26] is 10(3)%, with the IQCD values lying uniformly below our curves. No further information on  $B_c \rightarrow \eta_c$  is currently available from IQCD. Here, therefore, the interpolations we provide for our calculated transition form factors can be valuable in analysing future experimental data on the related transitions.

Working with our predictions and using Eqs. (5)–(8) evaluated with empirical lepton and meson masses, we obtain the  $B_c \rightarrow \eta_c$  branching fractions reported in Table 5A. Our results match well with other contemporary estimates.

Similarly, our predictions for the  $B_c \rightarrow J/\psi$  semileptonic transition form factors are given by Eq. (15) combined with the appropriate masses in Tables 1, 3 and coefficients listed in Table 2. The maximum recoil ( $t = 0$ ) value of each form factor is listed in Table 4, compared with recent continuum and lattice estimates. Once again, as highlighted by Fig. 2, different approaches produce a range of  $t = 0$  form factor values; but there is no significant tension, with all values falling within  $\lesssim 15\%$  of their respective means.

Our  $B_c \rightarrow J/\psi$  transition form factors are depicted in Figs. 4. Comparing with IQCD results [10], despite minor qualitative differences, most notably concerning  $V^{B_c \rightarrow J/\psi}(t)$  in Fig. 4B, there is semi-quantitative agreement. The interpolations we provide for our calculated transition form factors could be used to reduce a dominant systematic error in the extraction of  $R_{J/\psi}$

Table 5: Branching fractions calculated using our predictions for the semileptonic transition form factors in Eqs. (5)–(8) and empirical lepton and meson masses: (A)  $B_c \rightarrow \eta_c$ ; and (B)  $B_c \rightarrow J/\psi$ . Two uncertainties are listed with our results: first –  $1\sigma$  SPM uncertainty; second – from error on  $|V_{cb}|$ . Column 3 reports the ratio of the first two columns:  $|V_{cb}|$  cancels. Comparisons are provided with other analyses: quark model (QM) [11, 12]; phenomenology (ph) [13]; sum rules (SR) [14] modelling based on perturbative QCD (mpQCD) [15]; Salpeter equation (iBS) [16]; and IQCD [9, 10]. (No IQCD results are available for inclusion in Panel A.) As additional context, we list an unweighted average value for each quantity, evaluated with our prediction excluded (mean-e) and included (mean-i). Branching fractions are to be multiplied by  $10^{-3}$ .

A	$\mathcal{B}_{B_c \rightarrow \eta_c \mu \nu_\mu}$	$\mathcal{B}_{B_c \rightarrow \eta_c \tau \nu_\tau}$	$R_{\eta_c}$
herein	8.10(45)(55)	2.54(10)(17)	0.31(2)
QM [11, 12]	9.5(1.9)	2.4(0.5)	0.25(7)
ph [13]	6.6(0.2)		0.31(1)
SR [14]	8.2(1.2)	2.6(0.6)	0.32(2)
mpQCD [15]	7.8(1.7)	2.4(0.4)	0.31(1)
iBS [16]	5.3(2.2)	2.2(0.7)	0.38(4)
mean-e	7.5(1.6)	2.4(0.2)	0.31(4)
mean-i	7.6(1.5)	2.4(0.2)	0.31(4)

B	$\mathcal{B}_{B_c \rightarrow J/\psi \mu \nu_\mu}$	$\mathcal{B}_{B_c \rightarrow J/\psi \tau \nu_\tau}$	$R_{J/\psi}$
herein	17.2(1.9)(1.2)	4.17(66)(28)	0.24(5)
QM [11, 12]	16.7(3.3)	4.0(0.8)	0.24(7)
ph [13]	14.4(0.2)		0.26(1)
SR [14]	22.4(5.3)	5.3(1.5)	0.23(1)
mpQCD [15]	14.1(2.5)	3.8(0.6)	0.27(1)
iBS [16]	16.2(0.5)	4.3(0.1)	0.27(1)
IQCD [9, 10]	15.0(1.1)(1.0)		0.258(4)
mean-e	16.5(3.1)	4.4(0.7)	0.25(2)
mean-i	16.6(2.8)	4.3(0.6)	0.25(2)

from experiment [8], paving the way to improved precision and a more stringent test of the Standard Model.

Using Eqs. (5)–(8) evaluated with empirical lepton and meson masses and our predictions in Figs. 4, we obtain the  $B_c \rightarrow J/\psi$  branching fractions reported in Table 5B. Our results accord well with other contemporary estimates.

## 6. Conclusions and Perspectives

We employed a systematic, symmetry-preserving approach to the continuum strong-interaction bound-state problem in the Standard Model to calculate the semileptonic  $B_c \rightarrow \eta_c, J/\psi$  transition form factors on the entire physical kinematic domain. The framework [Sec. 3] has been used successfully to unify the properties of mesons and baryons with 0 – 3 heavy-quarks; and from this foundation, we arrived at an array of parameter-free predictions, including the branching fractions  $\mathcal{B}_{B_c \rightarrow \eta_c \ell \nu_\ell}$ ,  $\mathcal{B}_{B_c \rightarrow J/\psi \ell \nu_\ell}$ ,  $\ell = \mu, \tau$  [Sec. 5].

A key result of our analysis is highlighted by Fig. 1. Namely, contemporary Standard Model calculations of the ratio  $R_{J/\psi}$  in Eq. (2) are in agreement. Combined via the mean of their central values, they produce  $R_{J/\psi} = 0.253(16)$ , which is approximately  $2\sigma$  below the empirical result reported in Ref. [8]. If subsequent, precision experiments do not lead to a substantially lower central value, then one may conclude that lepton flavour

universality is violated in semileptonic  $B_c \rightarrow J/\psi$  decays. However, the precision of existing empirical information is insufficient to support such a claim. Moreover, a compelling case could only be compiled by including information on semileptonic  $B_c \rightarrow \eta_c$  decays. We predict  $R_{\eta_c} = 0.313(22)$ ; and the mean obtained from modern continuum analyses is 0.31(4) [Table 5A].

Natural extensions of this work include kindred analyses of  $b \rightarrow c$  transitions in the semileptonic decays of  $B_{(s)}$  mesons with  $D_{(s)}^{(*)}$  mesons in the final-state. Existing surveys of Standard Model theory estimates of the “ $R$ ” ratios associated with these additional processes yield values similar to those discussed herein, with the result for the pseudoscalar-meson final-state being  $\sim 15\%$  greater than that for the vector-meson final-state [69, 70]. Augmenting such analyses via the parameter-free unification of the results obtained herein with predictions for these other “ $R$ ” ratios should serve to increase confidence in Standard Model predictions and strengthen any case for or against lepton flavour universality in Nature. Furthermore, one could expand the coverage of our study to include a wider range of measurable quantities [4, 11], providing additional benchmarks for Standard Model tests in  $B_c$  decays.

**Acknowledgments** — We are grateful for constructive comments from X.-W. Kang and Z.-N. Xu; and to H.-S. Zong for friendship and guidance until his untimely death before this study was completed. Work supported by: Nanjing University Innovation Programme for PhD candidates; National Natural Science Foundation of China (under Grant No. 11805097); Jiangsu Provincial Natural Science Foundation of China (under Grant No. BK20180323); and STRONG-2020 “The strong interaction at the frontier of knowledge: fundamental research and applications”, which received funding from the European Union’s Horizon 2020 research and innovation programme under grant agreement No 824093.

## References

- [1] F. Abe, et al., Observation of  $B_c$  mesons in  $p\bar{p}$  collisions at  $\sqrt{s} = 1.8$  TeV, Phys. Rev. D 58 (1998) 112004.
- [2] P. Zyla, et al., Review of Particle Physics, PTEP 2020 (2020) 083C01.
- [3] N. Barik, S. Naimuddin, P. C. Dash, S. Kar, Semileptonic decays of the  $B_c$  meson, Phys. Rev. D 80 (2009) 074005.
- [4] L. Zhang, X.-W. Kang, X.-H. Guo, L.-Y. Dai, T. Luo, C. Wang, A comprehensive study on the semileptonic decay of heavy flavor mesons, JHEP 02 (2021) 179.
- [5] Z.-N. Xu, Z.-F. Cui, C. D. Roberts, C. Xu, Heavy+light pseudoscalar meson semileptonic transitions – arXiv:2103.15964 [hep-ph].
- [6] D. Scora, N. Isgur, Semileptonic meson decays in the quark model: An update, Phys. Rev. D 52 (1995) 2783–2812.
- [7] I. P. Gouz, V. V. Kiselev, A. K. Likhoded, V. I. Romanovsky, O. P. Yushchenko, Prospects for the  $B_c$  studies at LHCb, Phys. Atom. Nucl. 67 (2004) 1559–1570.
- [8] R. Aaij, et al., Measurement of the ratio of branching fractions  $\mathcal{B}(B_c^+ \rightarrow J/\psi \tau^+ \nu_\tau)/\mathcal{B}(B_c^+ \rightarrow J/\psi \mu^+ \nu_\mu)$ , Phys. Rev. Lett. 120 (12) (2018) 121801.
- [9] J. Harrison, C. T. H. Davies, A. Lytle,  $R(J/\psi)$  and  $B_c^- \rightarrow J/\psi \ell^- \bar{\nu}_\ell$  Lepton Flavor Universality Violating Observables from Lattice QCD, Phys. Rev. Lett. 125 (22) (2020) 222003.
- [10] J. Harrison, C. T. H. Davies, A. Lytle,  $B_c \rightarrow J/\psi$  form factors for the full  $q^2$  range from lattice QCD, Phys. Rev. D 102 (2020) 094518.
- [11] C.-T. Tran, M. A. Ivanov, J. G. Körner, P. Santorelli, Implications of new physics in the decays  $B_c \rightarrow (J/\psi, \eta_c)\tau\nu$ , Phys. Rev. D 97 (2018) 054014.

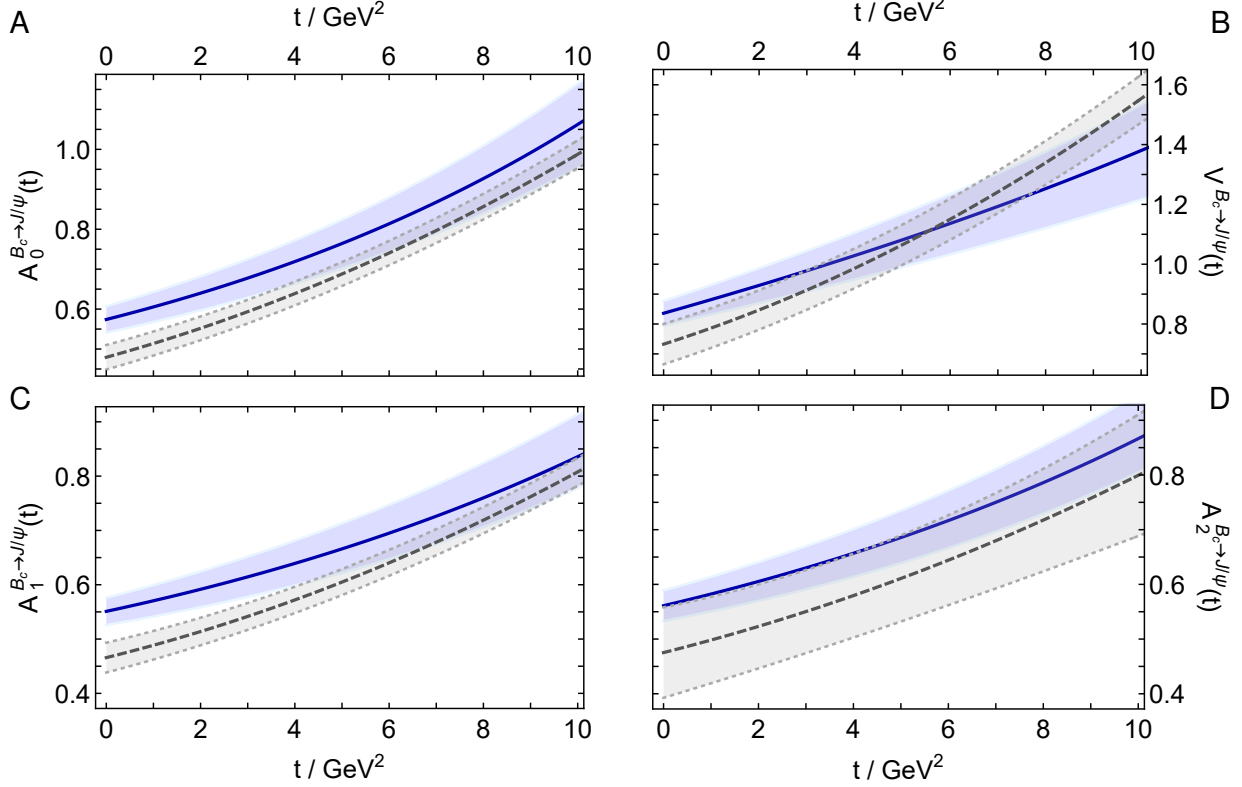


Figure 4: Predicted  $B_c \rightarrow J/\psi$  semileptonic transition form factors – solid blue curves within like-coloured bands, which express the  $1\sigma$  uncertainty on our SPM results. Comparable IQCD results from Ref. [10] – dashed grey curves within like-coloured bands.

- [12] A. Issadykov, M. A. Ivanov, The decays  $B_c \rightarrow J/\psi + \bar{\ell}\nu_\ell$  and  $B_c \rightarrow J/\psi + \pi(K)$  in covariant confined quark model, *Phys. Lett. B* 783 (2018) 178–182.
- [13] W. Wang, R. Zhu, Model independent investigation of the  $R_{J/\psi, \eta_c}$  and ratios of decay widths of semileptonic  $B_c$  decays into a P-wave charmonium, *Int. J. Mod. Phys. A* 34 (31) (2019) 1950195.
- [14] D. Lejnak, B. Melic, M. Patra, On lepton flavour universality in semileptonic  $B_c \rightarrow \eta_c, J/\psi$  decays, *JHEP* 05 (2019) 094.
- [15] X.-Q. Hu, S.-P. Jin, Z.-J. Xiao, Semileptonic decays  $B_c \rightarrow (\eta_c, J/\psi)\bar{\nu}_l$  in the ‘‘PQCD + Lattice’’ approach, *Chin. Phys. C* 44 (2) (2020) 023104.
- [16] T. Zhou, T. Wang, Y. Jiang, X.-Z. Tan, G. Li, G.-L. Wang, Relativistic calculations of  $R(D^{(*)})$ ,  $R(D_s^{(*)})$ ,  $R(\eta_c)$  and  $R(J/\psi)$ , *Int. J. Mod. Phys. A* 35 (17) (2020) 2050076.
- [17] J. P. Lees, et al., Measurement of an Excess of  $\bar{B} \rightarrow D^{(*)}\tau^-\bar{\nu}_\tau$  Decays and Implications for Charged Higgs Bosons, *Phys. Rev. D* 88 (7) (2013) 072012.
- [18] M. Huschle, et al., Measurement of the branching ratio of  $\bar{B} \rightarrow D^{(*)}\tau^-\bar{\nu}_\tau$  relative to  $\bar{B} \rightarrow D^{(*)}\ell^-\bar{\nu}_\ell$  decays with hadronic tagging at Belle, *Phys. Rev. D* 92 (7) (2015) 072014.
- [19] R. Aaij, et al., Measurement of the ratio of branching fractions  $\mathcal{B}(\bar{B}^0 \rightarrow D^{*+}\tau^-\bar{\nu}_\tau)/\mathcal{B}(\bar{B}^0 \rightarrow D^{*+}\mu^-\bar{\nu}_\mu)$ , *Phys. Rev. Lett.* 115 (11) (2015) 111803, [Erratum: *Phys. Rev. Lett.* 115, 159901 (2015)].
- [20] Y. Sato, et al., Measurement of the branching ratio of  $\bar{B}^0 \rightarrow D^{*+}\tau^-\bar{\nu}_\tau$  relative to  $\bar{B}^0 \rightarrow D^{*+}\ell^-\bar{\nu}_\ell$  decays with a semileptonic tagging method, *Phys. Rev. D* 94 (7) (2016) 072007.
- [21] S. Hirose, et al., Measurement of the  $\tau$  lepton polarization and  $R(D^*)$  in the decay  $\bar{B} \rightarrow D^*\tau^-\bar{\nu}_\tau$ , *Phys. Rev. Lett.* 118 (21) (2017) 211801.
- [22] R. Aaij, et al., Measurement of the ratio of the  $B^0 \rightarrow D^{*+}\tau^+\nu_\tau$  and  $B^0 \rightarrow D^{*+}\mu^+\nu_\mu$  branching fractions using three-prong  $\tau$ -lepton decays, *Phys. Rev. Lett.* 120 (17) (2018) 171802.
- [23] R. Aaij, et al., Test of lepton universality in beauty-quark decays.
- [24] A. Berns, H. Lamm, Model-Independent Prediction of  $R(\eta_c)$ , *JHEP* 12 (2018) 114.
- [25] T. D. Cohen, H. Lamm, R. F. Lebed, Precision Model-Independent Bounds from Global Analysis of  $b \rightarrow c\ell\nu$  Form Factors, *Phys. Rev. D* 100 (2019) 094503.
- [26] B. Colquhoun, C. Davies, J. Koponen, A. Lytle, C. McNeile,  $B_c$  decays from highly improved staggered quarks and NRQCD, *PoS LATTICE2016* (2016) 281.
- [27] T. Horn, C. D. Roberts, The pion: an enigma within the Standard Model, *J. Phys. G* 43 (2016) 073001.
- [28] G. Eichmann, H. Sanchis-Alepuz, R. Williams, R. Alkofer, C. S. Fischer, Baryons as relativistic three-quark bound states, *Prog. Part. Nucl. Phys.* 91 (2016) 1–100.
- [29] C. S. Fischer, QCD at finite temperature and chemical potential from Dyson–Schwinger equations, *Prog. Part. Nucl. Phys.* 105 (2019) 1–60.
- [30] S.-X. Qin, C. D. Roberts, Impressions of the Continuum Bound State Problem in QCD, *Chin. Phys. Lett.* 37 (12) (2020) 121201.
- [31] S.-X. Qin, L. Chang, Y.-X. Liu, C. D. Roberts, D. J. Wilson, Interaction model for the gap equation, *Phys. Rev. C* 84 (2011) 042202(R).
- [32] S.-X. Qin, L. Chang, Y.-x. Liu, C. D. Roberts, D. J. Wilson, Investigation of rainbow-ladder truncation for excited and exotic mesons, *Phys. Rev. C* 85 (2012) 035202.
- [33] S.-X. Qin, C. D. Roberts, S. M. Schmidt, Poincaré-covariant analysis of heavy-quark baryons, *Phys. Rev. D* 97 (2018) 114017.
- [34] D. Binosi, L. Chang, J. Papavassiliou, C. D. Roberts, Bridging a gap between continuum-QCD and ab initio predictions of hadron observables, *Phys. Lett. B* 742 (2015) 183–188.
- [35] Q.-W. Wang, S.-X. Qin, C. D. Roberts, S. M. Schmidt, Proton tensor charges from a Poincaré-covariant Faddeev equation, *Phys. Rev. D* 98 (2018) 054019.
- [36] M. Ding, K. Raya, A. Bashir, D. Binosi, L. Chang, M. Chen, C. D. Roberts,  $\gamma^*\gamma \rightarrow \eta, \eta'$  transition form factors, *Phys. Rev. D* 99 (2019) 014014.
- [37] D. Binosi, L. Chang, M. Ding, F. Gao, J. Papavassiliou, C. D. Roberts, Distribution Amplitudes of Heavy-Light Mesons, *Phys. Lett. B* 790 (2019) 257–262.
- [38] S.-X. Qin, C. D. Roberts, S. M. Schmidt, Spectrum of light- and heavy-baryons, *Few Body Syst.* 60 (2019) 26.
- [39] Y.-Z. Xu, D. Binosi, Z.-F. Cui, B.-L. Li, C. D. Roberts, S.-S. Xu, H.-S. Zong, Elastic electromagnetic form factors of vector mesons, *Phys. Rev.*

- D 100 (2019) 114038.
- [40] Z.-Q. Yao, D. Binosi, Z.-F. Cui, C. D. Roberts, S.-S. Xu, H.-S. Zong, Semileptonic decays of  $D_{(s)}$  mesons, *Phys. Rev. D* 102 (2020) 014007.
- [41] H. J. Munczek, Dynamical chiral symmetry breaking, Goldstone's theorem and the consistency of the Schwinger-Dyson and Bethe-Salpeter Equations, *Phys. Rev. D* 52 (1995) 4736–4740.
- [42] A. Bender, C. D. Roberts, L. von Smekal, Goldstone Theorem and Di-quark Confinement Beyond Rainbow-Ladder Approximation, *Phys. Lett. B* 380 (1996) 7–12.
- [43] C.-R. Ji, P. Maris,  $K_{\ell 3}$  transition form-factors, *Phys. Rev. D* 64 (2001) 014032.
- [44] L. Chang, Y.-X. Liu, C. D. Roberts, Y.-M. Shi, W.-M. Sun, H.-S. Zong, Chiral susceptibility and the scalar Ward identity, *Phys. Rev. C* 79 (2009) 035209.
- [45] D. Binosi, C. D. Roberts, J. Rodríguez-Quintero, Scale-setting, flavour dependence and chiral symmetry restoration, *Phys. Rev. D* 95 (2017) 114009.
- [46] F. Gao, S.-X. Qin, C. D. Roberts, J. Rodríguez-Quintero, Locating the Gribov horizon, *Phys. Rev. D* 97 (2018) 034010.
- [47] Z.-F. Cui, J.-L. Zhang, D. Binosi, F. de Soto, C. Mezrag, J. Papavassiliou, C. D. Roberts, J. Rodríguez-Quintero, J. Segovia, S. Zafeiropoulos, Effective charge from lattice QCD, *Chin. Phys. C* 44 (2020) 083102.
- [48] A. Kızılersü, O. Oliveira, P. J. Silva, J.-I. Skullerud, A. Sternbeck, Quark-gluon vertex from Nf=2 lattice QCD – arXiv:2103.02945 [hep-lat].
- [49] C. D. Roberts, Empirical Consequences of Emergent Mass, *Symmetry* 12 (2020) 1468.
- [50] C. D. Roberts, D. G. Richards, T. Horn, L. Chang, *Insights into the Emergence of Mass from Studies of Pion and Kaon Structure* – arXiv:2102.01765 [hep-ph], *Prog. Part. Nucl. Phys. in press*.
- [51] C. T. H. Davies, et al., Update: Precision  $D_s$  decay constant from full lattice QCD using very fine lattices, *Phys. Rev. D* 82 (2010) 114504.
- [52] C. McNeile, C. T. H. Davies, E. Follana, K. Hornbostel, G. P. Lepage, Heavy meson masses and decay constants from relativistic heavy quarks in full lattice QCD, *Phys. Rev. D* 86 (2012) 074503.
- [53] B. Colquhoun, C. T. H. Davies, R. J. Dowdall, J. Kettle, J. Koponen, G. P. Lepage, A. T. Lytle, B-meson decay constants: a more complete picture from full lattice QCD, *Phys. Rev. D* 91 (2015) 114509.
- [54] P. Maris, C. D. Roberts,  $\pi$  and  $K$  meson Bethe-Salpeter amplitudes, *Phys. Rev. C* 56 (1997) 3369–3383.
- [55] A. Windisch, Analytic properties of the quark propagator from an effective infrared interaction model, *Phys. Rev. C* 95 (2017) 045204.
- [56] L. Chang, I. C. Cloet, C. D. Roberts, S. M. Schmidt, P. C. Tandy, Pion electromagnetic form factor at spacelike momenta, *Phys. Rev. Lett.* 111 (2013) 141802.
- [57] N. Nakanishi, A General survey of the theory of the Bethe-Salpeter equation, *Prog. Theor. Phys. Suppl.* 43 (1969) 1–81.
- [58] C. Chen, Y. Lu, D. Binosi, C. D. Roberts, J. Rodríguez-Quintero, J. Segovia, Nucleon-to-Roper electromagnetic transition form factors at large  $Q^2$ , *Phys. Rev. D* 99 (2019) 034013.
- [59] D. Binosi, R.-A. Tripolt, Spectral functions of confined particles, *Phys. Lett. B* 801 (2020) 135171.
- [60] M. Ding, K. Raya, D. Binosi, L. Chang, C. D. Roberts, S. M. Schmidt, Symmetry, symmetry breaking, and pion parton distributions, *Phys. Rev. D* 101 (5) (2020) 054014.
- [61] M. Ding, K. Raya, D. Binosi, L. Chang, C. D. Roberts, S. M. Schmidt, Drawing insights from pion parton distributions, *Chin. Phys. C (Lett.)* 44 (2020) 031002.
- [62] E. V. Souza, M. Narciso Ferreira, A. C. Aguilar, J. Papavassiliou, C. D. Roberts, S.-S. Xu, Pseudoscalar glueball mass: a window on three-gluon interactions, *Eur. Phys. J. A (Lett.)* 56 (2020) 25.
- [63] Z.-F. Cui, C. Chen, D. Binosi, F. de Soto, C. D. Roberts, J. Rodríguez-Quintero, S. M. Schmidt, J. Segovia, Nucleon elastic form factors at accessible large spacelike momenta, *Phys. Rev. D* 102 (2020) 014043.
- [64] M. Q. Huber, C. S. Fischer, H. Sanchis-Alepuz, Spectrum of scalar and pseudoscalar glueballs from functional methods, *Eur. Phys. J. C* 80 (11) (2020) 1077.
- [65] Z.-F. Cui, D. Binosi, C. D. Roberts, S. M. Schmidt, *Fresh extraction of the proton charge radius from electron scattering* – arXiv:2102.01180 [hep-ph].
- [66] L. Schlessinger, C. Schwartz, Analyticity as a Useful Computation Tool, *Phys. Rev. Lett.* 16 (1966) 1173–1174.
- [67] L. Schlessinger, Use of Analyticity in the Calculation of Nonrelativistic Scattering Amplitudes, *Phys. Rev.* 167 (1968) 1411–1423.
- [68] N. Mathur, M. Padmanath, S. Mondal, Precise predictions of charmed-bottom hadrons from lattice QCD, *Phys. Rev. Lett.* 121 (20) 202002.
- [69] X.-Q. Hu, S.-P. Jin, Z.-J. Xiao, Semileptonic decays  $B/B_s \rightarrow (D^{(*)}, D_s^{(*)})\ell\nu_\ell$  in the PQCD approach with the lattice QCD input, *Chin. Phys. C* 44 (5) (2020) 053102.
- [70] P. Gambino, et al., Challenges in semileptonic  $B$  decays, *Eur. Phys. J. C* 80 (10) (2020) 966.